JOURNAL OF GUIDANCE, CONTROL, AND DYNAMICS
Vol. 17, No. 6, November–December 1994

Quantification of Parametric Uncertainty via an Interval Model

Jiann-Shiun Lew* and Lee H. Keel*
Tennessee State University, Nashville, Tennessee 37203-3401
and
Jer-Nan Juang†
NASA Langley Research Center, Hampton, Virginia 23681

The quantification of model uncertainty becomes increasingly important as robust control is an important tool for control system design and analysis. This paper presents an algorithm to characterize the model uncertainty in terms of parametric and nonparametric uncertainties directly from input/output data. We focus on the quantification of parametric uncertainty, which is represented as an interval system of the transfer function. Using this family of transfer functions (interval system), we give complete analysis of the system. A numerical example is used to demonstrate and verify the developed algorithm. The example illustrates the application of recently developed interval system techniques to the identified interval models.

Nomenclature

A, B, C, D	= matrices of state-space model
a, b	= parameters of model structure 3
G	= interval model
g	= transfer function
g_e	= estimated spectral error of nominal model
$\hat{g}$	= estimated spectrum
N	= number of time-domain data
N_p	= number of frequency points chosen for parametric uncertainty
N_s	= number of data for each spectrum
$\boldsymbol{p}$	= parameter vector of transfer function
p_n	= number of frequency ranges chosen for parametric uncertainty
q, r	= polynomials of model structure 2
q_0, r_0	= denominator and numerator of nominal model
S, U, V	= matrices of singular-value decomposition
T	= discrete-time interval
u	= input data
$\boldsymbol{w}$	= frequency range chosen for parametric uncertainty
Y	= output of interval model with nonparametric error bound
y	= output data
$\hat{y}, y_e$	= output and output error of identified model
α, β	= parameters of model structures 1 and 2
Δ	= error operator
$\boldsymbol{\Delta}_d, \boldsymbol{\Delta}_n$	= denominator and numerator parameter error matrices
$\boldsymbol{\Delta}d, \boldsymbol{\Delta}n$	= denominator and numerator parameter error vectors
ΔG	= error bound transfer function for nonparametric uncertainty
Δg	= spectral error due to model error $\Delta \boldsymbol{p}_1$
$\Delta g^{\perp}$	= orthogonal error of spectral error Δg
$\Delta \boldsymbol{p}_1, \Delta \boldsymbol{p}_2$	= sensitivity vectors due to spectral errors
$\boldsymbol{\Delta}_P$	= parameter error matrix
μ, ν	= coefficients of sensitivity vectors
ω	= frequency

Subscript

s	= continuous system

Superscripts

f	= discrete Fourier transform
0	= nominal model
$-, +$	= lower and upper bounds

Introduction

FOR the last decade, the problem of quantifying model uncertainty has received a special attention by many researchers in both robust control and system identification communities. In recent years, several different approaches have been developed to deal with this problem.[1–4] Among them, the H_∞ approach is the most popular, and its objective is to obtain a nominal model and its corresponding H_∞ error bound.[1,2]

In general, a large flexible structure has hundreds of modes.[5] The model used for a control design is usually chosen to be linear and includes only few low-frequency modes of interest. For flexible structures with low damping, the frequency spectrum describing the model error has peaks close to the natural frequencies of the identified modes. Due to these peaks, it may be necessary to find an H_∞ error transfer function with large magnitude in the ranges of low frequencies to bound them. Clearly the choice of error transfer function with large H_∞ magnitude results in an H_∞ control design with poor performance satisfying the required robustness condition.

In this paper, we attempt to overcome this drawback by introducing both parametric and nonparametric (i.e., H_∞) uncertainties. The parametric uncertainty is used to cover the model error spectrum around the natural frequencies of the identified modes. The parametric uncertainty is determined by quantifying the parameter error of the identified parameters. The error due to the unmodeled high-frequency modes and measurement noise is considered as nonparametric uncertainty. A transfer function is designed to bound the nonparametric uncertainty. Some justification of combining parametric and nonparametric uncertainties are as follows:

1) It is natural to consider the parametric error of the identified modes as parametric uncertainty rather than nonparametric uncertainty.

2) It is intuitively logical to cover the unmodeled high-frequency modes by using nonparametric uncertainty instead of parametric uncertainty. Otherwise, significantly large parametric uncertainty is needed to cover the unmodeled high-frequency modes.

3) The measurement noise represents infinite modes uniformly distributed in the frequency domain. If the spectrum of measurement noise is not negligible, it is unrealistic to use the parametric uncertainty of finite identified modes to cover the measurement noise.

In this paper, we use the framework of interval systems to represent parametric uncertainty. The interval system is the system whose

Received June 15, 1993; revision received May 24, 1994; accepted for publication May 25, 1994.

*Assistant Professor, Center of Excellence in Information Systems. Member AIAA.

†Principal Scientist, Spacecraft Dynamics Branch. Fellow AIAA.

transfer function coefficients are functions of bounded parameters. In particular, if coefficients are linear combinations of bounded parameters, we call this linear interval systems. Since the celebrated theorem of Kharitonov[6] and its extension,[7] many important properties of interval systems became widely known.[7–9] The advantage of using such an interval transfer function model is that it provides us complete analysis of the entire family of systems belonging to the interval model. It includes the frequency-domain behavior as well as regions in which the roots of the family lie.[10] In this paper, the Mini-Mast[5] is used to illustrate the algorithm based on the important properties of interval systems reported in Refs. 7–9.

Model Structures

Let us consider a set of finite measured sample data

$$\{y(k),\ u(k):\ k = 1, \ldots, N\} \tag{1}$$

where $u(k)$ and $y(k)$ represent discrete points of input and output data of a system, respectively. Clearly, there is no single linear time-invariant system whose transfer function represents exactly the relationship between $u(k)$ and $y(k)$ due to a variety of uncertainties such as nonlinearity, noise, etc. Thus, our aim is to construct a class of linear time-invariant systems that contains the complete behavior of the system observed by $u(k)$ and $y(k)$. This task may be accomplished by determining a reasonably parametrized interval model $G(z,\ \boldsymbol{p})$ and its corresponding error bound transfer function ΔG so that the output $y(k)$ belongs to the class of output $Y(k)$. We depict this relation in Fig. 1.

The most common structure of interval transfer functions used in parametric robust control is described as follows:

Model structure 1:

$$G(z,\ \boldsymbol{p}) = \left\{ g(z,\ \boldsymbol{p}) = \frac{r_0(z) + \sum_{i=0}^{m} \alpha_i z^i}{q_0(z) + \sum_{i=0}^{m-1} \beta_i z^i} :\ \alpha_i \in [\alpha_i^- \alpha_i^+],\ \beta_i \in [\beta_i^- \beta_i^+] \right\} \tag{2}$$

where the parameter vector is defined as

$$\boldsymbol{p} = [\beta_{m-1}, \ldots, \beta_0, \alpha_m, \ldots, \alpha_0]^T \tag{3}$$

where the mth-order polynomial $r_0(z)$ and the monic polynomial $q_0(z)$ are the numerator and denominator of the nominal model, respectively. The variables α_i and β_i represent the parametric uncertainty. This structure has been used to model the parametric uncertainty for continuous systems.[11]

Another model structure introduced in this paper is described as follows:

Model structure 2:

$$G(z,\ \boldsymbol{p}) = \left\{ g(z,\boldsymbol{p}) = \frac{r_0(z) + \sum_{i=1}^{m+1} \alpha_i r_i(z)}{q_0(z) + \sum_{i=1}^{m} \beta_i q_i(z)} :\ \alpha_i \in [\alpha_i^- \alpha_i^+],\ \beta_i \in [\beta_i^- \beta_i^+] \right\} \tag{4}$$

where $\{r_1(z), r_2(z), \ldots, r_{m+1}(z)\}$ is a basis for the polynomials of degree m and $\{q_1(z), q_2(z), \ldots, q_m(z)\}$ is a basis for the polynomials of degree $m - 1$. Later, a technique based on the singular-value decomposition (SVD) will be developed to obtain these two bases. Note that the model structure 1 is a special case of the model structure 2, which has more degrees of freedom. Finally, we introduce one more model structure that may be useful for many design practices:

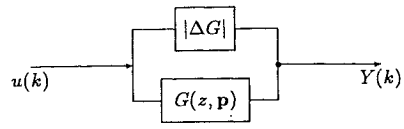

Fig. 1 Model structure with uncertainty.

Model structure 3:

$$G(z,\boldsymbol{p}) = \left\{ b + \sum_{i=1}^{k_1} \frac{b_i}{z + a_i} + \sum_{i=1}^{k_2} \frac{b_{1i} z + b_{0i}}{z^2 + a_{1i} z + a_{0i}} :\ b \in [b^-, b^+],\ b_i \in [b_i^-, b_i^+], a_i \in [a_i^-, a_i^+],\ b_{jk} \in [b_{jk}^-, b_{jk}^+], a_{jk} \in [a_{jk}^-, a_{jk}^+] \right\} \tag{5}$$

This model structure has the form of partial fractions. In this paper, the model structure 3 will not be used. However, some discussion will be given along with the example.

Problem Approach

The algorithm to quantify parametric and nonparametric uncertainties starts with identifying a nominal discrete-time model.

Identified Nominal Model

The observer/Kalman filter identification (OKID) algorithm[12,13] is an effective system identification tool that produces a discrete state-space model from the given input and output testing data. In this paper, the OKID is used to identify a nominal transfer function denoted by

$$g(z,\boldsymbol{p}^0) = C^0(zI - A^0)^{-1}B^0 + D^0 = \frac{n_m^0 z^m + n_{m-1}^0 z^{m-1} + \cdots + n_0^0}{z^m + d_{m-1}^0 z^{m-1} + \cdots + d_0^0} \tag{6}$$

where A^0, B^0, C^0, and D^0 are OKID-identified system matrices and the parameter vector of the nominal model is specified as

$$\boldsymbol{p}^0 = [d_{m-1}^0, \ldots, d_0^0, n_m^0, \ldots, n_0^0]^T. \tag{7}$$

Model Error Estimation

The output error of the identified model is defined as

$$y_e(k) := y(k) - \hat{y}(k) \tag{8}$$

where $\hat{y}(k)$ denotes the output signal obtained by driving the OKID-identified model $g(z,\ \boldsymbol{p}^0)$ with the input $u(k), k = 1, \ldots, N$. The model error in the frequency domain is estimated as the ratio of the DFT (discrete Fourier transforms) of the output error y_e and the input u,[1,14]

$$g_e(z) := \frac{y_e^f(z)}{u^f(z)}, \qquad u^f(z) := \mathrm{DFT}(u)$$
$$y_e^f(z) := \mathrm{DFT}(y_e) \tag{9}$$

In this paper, it is assumed that the estimated model error $g_e(z)$ is treated as the true model error of the identified nominal model for the given input and output data. Therefore, the spectrum

$$\hat{g}(z) = g(z,\ \boldsymbol{p}^0) + g_e(z) \tag{10}$$

represents the overall frequency-domain data estimated from the time-domain input and output data. Notation like $\hat{g}(z)$ that consists of only one variable z represents the spectrum generated from *data*. Now the estimated model error g_e is separated into parametric and nonparametric uncertainties, which we discuss in the following sections.

Parametric Uncertainty Estimation

For parametric uncertainty, first we choose a set of reasonable ranges of frequencies in that the peak errors of g_e occur around the natural frequencies of the identified modes. Let these ranges of frequencies be

$$\boldsymbol{w}_i := \left[\boldsymbol{w}_i^-, \boldsymbol{w}_i^+\right], \qquad \boldsymbol{w}_i^- < \boldsymbol{w}_i^+, \qquad i = 1, 2, \ldots, p_n \tag{11}$$

where p_n denotes the number of error peaks and $\boldsymbol{w}_i^-$ and $\boldsymbol{w}_i^+$ are the lower and upper limits of the ith frequency range $\boldsymbol{w}_i$, respectively. Let N_p denote the total number of frequency points that belong to the frequency intervals $\boldsymbol{w}_i$ for $i = 1, 2, \ldots, p_n$.

We obtain the nominal model $g(z, \boldsymbol{p}^0)$, the estimated model error $g_e(z)$, and the chosen frequency points ω_η, where η is the index of the frequency point in Eq. (11). Then let i_γ ($\gamma = 1, 2, \ldots, N_p$) denote the index of η corresponding to the chosen frequency ω_η, i.e., $\omega_{i_\gamma} = \omega_\eta$. The next step is to estimate the parameter error due to the error $g_e(z_{i_\gamma})$ at each frequency ω_{i_γ}. The algorithm presented here estimates the parameter error by using the sensitivity criterion described below. To compute the sensitivity due to the error g_e at frequency ω_{i_γ}, we use the least-squares technique to obtain the identified model for the following spectrum:

$$\hat{g}^\gamma(z_k) = \begin{cases} g\left(z_k, \boldsymbol{p}^0\right), & \text{if } k = 1, \ldots, i_\gamma - 1, i_\gamma + 1, \ldots, N_s \\ \hat{g}(z_k), & \text{if } k = i_\gamma \end{cases} \tag{12}$$

where N_s is the number of spectral data. This frequency spectrum is identical to the spectrum $g(z, \boldsymbol{p}^0)$ of the identified nominal model except at the i_γth frequency point. The i_γth frequency point is replaced by the spectrum $\hat{g}(z)$ at the same frequency. As a result, we have N_p identified parameter vectors $\boldsymbol{p}_1^\gamma$ corresponding to N_p spectra, i.e.,

$$\{\hat{g}^\gamma(z_k), \quad k = 1, 2, \ldots, N_s, \quad \gamma = 1, 2, \ldots, N_p\}$$

$$\Downarrow \quad \text{transfer function realization}$$

$$\left\{\boldsymbol{p}_1^\gamma, \quad \gamma = 1, 2, \ldots, N_p\right\}$$

The parameter error of the γth realized transfer function is

$$\Delta\boldsymbol{p}_1^\gamma := \boldsymbol{p}_1^\gamma - \boldsymbol{p}^0 \tag{13}$$

and it is the parameter sensitivity due to the error g_e at $z_{i_\gamma} = e^{j\omega_{i_\gamma}T}$. This sensitivity $\Delta\boldsymbol{p}_1^i$ gives the weighting of the parameter error due to the model error g_e at z_{i_γ}.

Let the error at z_{i_γ} due to the parameter error $\Delta\boldsymbol{p}_1^\gamma$ be represented as

$$\Delta g^\gamma = g\left(z_{i_\gamma}, \boldsymbol{p}^0 + \Delta\boldsymbol{p}_1^\gamma\right) - g\left(z_{i_\gamma}, \boldsymbol{p}^0\right) \tag{14}$$

where

$$g(z, \boldsymbol{p}) = \frac{n_m z^m + n_{m-1} z^{m-1} + \cdots + n_0}{z^m + d_{m-1} z^{m-1} + \cdots + d_0} \tag{15}$$

and

$$\boldsymbol{p} = [d_{m-1}, \ldots, d_0, n_m, \ldots, n_0]^T \tag{16}$$

It is important to note that the error $g_e(z_{i_\gamma})$ defined in Eq. (9) may not be exactly in the direction of Δg^γ. This means that changing the parameter from $\boldsymbol{p}^0$ in the $\Delta\boldsymbol{p}_1^\gamma$ direction may not exactly capture the two-dimensional complex number $g_e(z_{i_\gamma})$ at z_{i_γ}. To exactly capture the model error, we introduce another parameter vector that represents the parameter sensitivity due to the orthogonal error of Δg^γ. Figure 2 shows the relationship between $g_e(z_{i_\gamma})$, Δg^γ, and $(\Delta g^\perp)^\gamma$. In Fig. 2, $\tau\Delta g^\gamma$ is the projection of $g_e(z_{i_\gamma})$ in the direction of Δg^γ. In general, the difference between $\tau\Delta g^\gamma$ and $g_e(z_{i_\gamma})$ is negligible. The magnitude of $g_e(z_{i_\gamma})$ is at least 10^2 times larger than the magnitude of $(\Delta g^\perp)^\gamma$. In order to obtain the parameter sensitivity with respect to the orthogonal error, we replace $g_e(z_{i_\gamma})$ in Eq. (10) by $(\Delta g^\perp)^\gamma$ and proceed to another realization procedure. From these realized model parameters, we obtain the parameter sensitivity due to the orthogonal error $(\Delta g^\perp)^\gamma$. This sensitivity is symbolized as

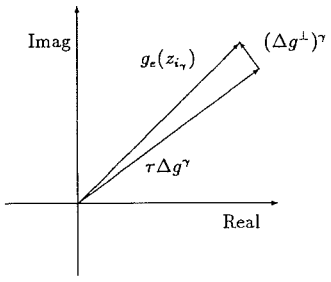

Fig. 2 Model error.

$\Delta\boldsymbol{p}_2^\gamma$. The two sensitivities $\Delta\boldsymbol{p}_1^\gamma$ and $\Delta\boldsymbol{p}_2^\gamma$ are used to generate the equation for the parameter error estimation as

$$\sum_{j=0}^{m-1}\left[g\left(z_{i_\gamma}, \boldsymbol{p}^0\right) + g_e(z_{i_\gamma})\right]\left(d_j^0 + \mu^\gamma\,\Delta d_{j1}^\gamma + \nu^\gamma\,\Delta d_{j2}^\gamma\right)z_{i_\gamma}^j$$

$$-\sum_{j=0}^{m}\left(n_j^0 + \mu^\gamma\Delta n_{j1}^\gamma + \nu^\gamma\Delta n_{j2}^\gamma\right)z_{i_\gamma}^j$$

$$= -\left[g\left(z_{i_\gamma}, \boldsymbol{p}^0\right) + g_e(z_{i_\gamma})\right]z_{i_\gamma}^m \tag{17}$$

where Δd_{j1}^γ and Δn_{j1}^γ are the elements of $\Delta\boldsymbol{p}_1^\gamma$ and Δd_{j2}^γ and Δn_{j2}^γ are the elements of $\Delta\boldsymbol{p}_2^\gamma$. This equation can be separated into real and imaginary parts to produce two linear equations with two unknowns, μ and ν. A unique solution $[\mu^\gamma\ \nu^\gamma]^T$ can be obtained to satisfy these two linear equations. The parameter error can then be computed as

$$\Delta\boldsymbol{p}^\gamma = \mu^\gamma\,\Delta\boldsymbol{p}_1^\gamma + \nu^\gamma\,\Delta\boldsymbol{p}_2^\gamma \tag{18}$$

This parameter error vector is the solution of Eq. (17) and exactly fits the model error g_e at z_{i_γ}. The γth realized parameter vector is expressed as

$$\boldsymbol{p}^\gamma = \boldsymbol{p}^0 + \Delta\boldsymbol{p}^\gamma. \tag{19}$$

The procedure is repeated for all $\gamma = 1, 2, \ldots, N_p$. As a result, we have N_p parameter error vectors $\Delta\boldsymbol{p}^\gamma$, $\gamma = 1, 2, \ldots, N_p$, where

$$\Delta\boldsymbol{p}^\gamma = \left[\Delta d_{m-1}^\gamma, \ldots, \Delta d_0^\gamma, \Delta n_m^\gamma, \ldots, \Delta n_0^\gamma\right]^T \tag{20}$$

Let the upper and lower bounds of the parameter uncertainty for model structure 1 be selected as

$$\begin{aligned} \alpha_j^- &:= \min\left\{\Delta n_j^1, \ldots, \Delta n_j^{N_p}, 0\right\} \\ \alpha_j^+ &:= \max\left\{\Delta n_j^1, \ldots, \Delta n_j^{N_p}, 0\right\} \\ \beta_k^- &:= \min\left\{\Delta d_k^1, \ldots, \Delta d_k^{N_p}, 0\right\} \\ \beta_k^+ &:= \max\left\{\Delta d_k^1, \ldots, \Delta d_k^{N_p}, 0\right\} \end{aligned} \tag{21}$$

for $j = 0, \ldots, m$, $k = 0, \ldots, m-1$. Here min and max represent the minimum and the maximum of the corresponding set of variables, respectively. For model structure 1, we also define the vectors of the limiting values of parameters:

$$\boldsymbol{p}^+ = \left[d_{m-1}^0 + \beta_{m-1}^+, \ldots, d_0^0 + \beta_0^+, n_m^0 + \alpha_m^+, \ldots, n_0^0 + \alpha_0^+\right]^T$$

$$\boldsymbol{p}^- = \left[d_{m-1}^0 + \beta_{m-1}^-, \ldots, d_0^0 + \beta_0^-, n_m^0 + \alpha_m^-, \ldots, n_0^0 + \alpha_0^-\right]^T \tag{22}$$

Now consider the model structure 2 in Eq. (4). Constructing an interval transfer function based on the model structure 2 is accomplished by selecting parameter intervals for α_k and β_k and determining polynomials $r_k(z)$ and $q_k(z)$ for all k. First form a matrix from all $\Delta\boldsymbol{p}^i$ for $i = 1, 2, \ldots, N_p$, where

$$\begin{aligned} \Delta_p &:= \left[\Delta\boldsymbol{p}^1 \quad \Delta\boldsymbol{p}^2 \cdots \Delta\boldsymbol{p}^{N_p}\right] \\ &:= \begin{bmatrix} \boldsymbol{\Delta d}_1 & \boldsymbol{\Delta d}_2 \cdots \boldsymbol{\Delta d}_{N_p} \\ \boldsymbol{\Delta n}_1 & \boldsymbol{\Delta n}_2 \cdots \boldsymbol{\Delta n}_{N_p} \end{bmatrix} \end{aligned} \tag{23}$$

The vector Δd_i is the denominator part of Δp^i and let

$$\Delta_d := \left[\, \Delta d_1 \;\; \Delta d_2 \cdots \Delta d_{N_p} \,\right] \tag{24}$$

which is an $m \times N_p$ matrix. Similarly, Δ_n can also be defined. Using the SVD[15] to factorize the matrix Δ_d yields

$$\Delta_d = USV^T, \qquad U = [U_1 \;\; U_2 \cdots U_m], \qquad V = \left[V_1 \;\; V_2 \cdots V_{N_p}\right] \tag{25}$$

where U and V are orthonormal matrices and S is a rectangular singular-value matrix. The corresponding coordinate vector of the error Δd_i relative to the basis $\{U_1, U_2, \ldots, U_m\}$ becomes

$$\Delta q_i = U^T \Delta d_i, \qquad i = 1, \ldots, N_p \tag{26}$$

The polynomials $q_i(z)$ of the model structure 2 are now composed of the basis vectors of U,

$$q_i(z) = \sum_{j=1}^{m} U_i(j) z^{m-j} \tag{27}$$

where $U_i(j)$ is the jth element of U_i. Finally, we determine the bounds for the corresponding polynomial $q_j(z)$ as

$$\begin{aligned} \beta_j^+ &= \max\{\Delta q_1(j), \ldots, \Delta q_{N_p}(j), 0\} \\ \beta_j^- &= \min\{\Delta q_1(j), \ldots, \Delta q_{N_p}(j), 0\} \end{aligned} \tag{28}$$

for $j = 1, \ldots, m$. Similarly, the SVD is also applied to Δ_n to produce $r_i(z), \alpha_i^-$, and α_i^+. The discrete-interval model for the model structure 2 is thus established.

For each identified model p^γ, one obtains a partial-fraction expansion model as shown in Eq. (5). To derive the model structure 3, the interval of each parameter is chosen as the range between the minimum and maximum of the corresponding realized parameters.

Nonparametric Uncertainty

In the H_∞ robust control design, the model error is treated as the nonparametric error and it is used to design an additive uncertainty weighting transfer function.[16] The model error g_e for the frequency points outside the ranges defined in Eq. (11) is considered resulting from nonparametric uncertainty. The problem is to find an error transfer function to bound this part model error, and it is beyond the scope of this paper.

Transfer to Continuous Model

For each identified discrete model described by p^γ, we can use the bilinear transformation

$$z = \frac{1 + (T/2)s}{1 - (T/2)s} \tag{29}$$

to obtain the corresponding continuous model described by p_s^γ. Then the γth continuous-model parameter error can be computed as

$$\Delta p_s^\gamma = p_s^\gamma - p_s^0 \tag{30}$$

where p_s^0 describes the continuous nominal model. Using the previous procedure, one can generate the continuous interval models from Δp_s^γ.

Numerical Example

We choose a finite element model of the Mini-Mast structure[5] to illustrate the algorithm developed in this paper. The Mini-Mast as shown in Fig. 3 was a 20.16-m-long deployable truss in the Structural Dynamics Research Laboratory at NASA Langley Research Center. It was used as a ground test article for research in the areas of structural analysis, system identification, and control of large space structures. For simplicity, the system model used in this example consists only of the first three low-frequency modes in one direction: two bending modes and one torsional mode with eigenvalues $-0.09059 \pm j5.0318$, $-0.3868 \pm j38.682$, and $-0.3291 \pm j27.420$, respectively. In addition, only a single input and a single output as shown in Fig. 3 are considered. In this paper, the measurement used for identification is the random input response of the following state-space model:

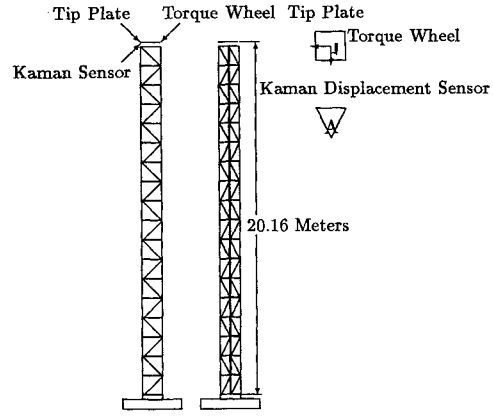

Fig. 3 Mini-Mast test article showing x torque wheel input and A displacement output.

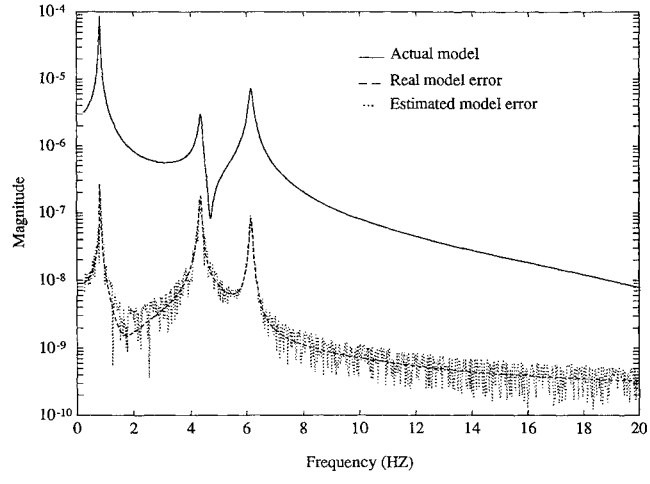

Fig. 4 Model error estimation.

$$\begin{aligned} x(k+1) &= Ax(k) + Bu(k) + w(k) \\ y(k) &= Cx(k) + Du(k) + v(k) \end{aligned} \tag{31}$$

where $[A\ B\ C\ D]$ is the simplified system model including only three modes as described above. Unless otherwise stated, the simplified system model is referred to as the "actual" model. The variables x, y, and u are state vector, output, and input, respectively. The variable w is the model error (process noise), which in real cases includes nonlinearity, disturbance, etc. The variable v is the measurement noise. The matrices A, B, C, and D and the characteristics of w and v can be found in Ref. 17. The first 2000 random input response data with sampling rate at 50 Hz are used for identification.

Model Error Estimation

In this section, we show the numerical model error estimation, i.e., Eq. (9). Assume that the actual model described by the parameter p is the true system model. A nominal model parameter p^0 is chosen with the "true" model error computed as the difference between the spectra of p and p^0. The output error is computed as the difference between the outputs obtained by driving the actual model and the nominal model with the same random input. The estimated model error g_e is computed as the ratio of the DFTs of the output error and the input. Figure 4 shows the magnitude plots of the actual model, the true model error, and the estimated model error. The estimated model error (dotted line) well represents the true model error (dashed line) in the frequency domain. Especially, the estimated error is coincident with the true error around the three peaks, which are the frequency ranges chosen for quantification of parametric uncertainty. Note that the true model error is not available in practice.

Table 1 Discrete model structure 1

		p	p^0	p^-	p^+
n_i	z^5	3.6867×10^{-8}	3.7102×10^{-8}	3.5890×10^{-8}	3.8703×10^{-8}
	z^4	-1.0500×10^{-7}	-1.0591×10^{-7}	-1.1274×10^{-7}	-1.0113×10^{-7}
	z^3	6.5855×10^{-8}	6.7430×10^{-8}	5.8963×10^{-8}	8.0038×10^{-8}
	z^2	6.4656×10^{-8}	6.3099×10^{-8}	5.0545×10^{-8}	7.1542×10^{-8}
	z^1	-1.0328×10^{-7}	-1.0242×10^{-7}	-1.0723×10^{-7}	-9.5691×10^{-8}
	z^0	3.6166×10^{-8}	3.5949×10^{-8}	3.4381×10^{-8}	3.7190×10^{-8}
d_i	z^5	−5.1015	−5.1017	−5.1025	−5.0998
	z^4	11.563	11.564	11.555	11.568
	z^3	−14.872	−14.874	−14.882	−14.858
	z^2	11.434	11.436	11.421	11.444
	z^1	−4.9897	−4.9911	−4.9952	−4.9828
	z^0	0.96826	0.96859	0.96671	0.96947

Table 2 Singular-value comparison

SVD no.	SVD(Δ_d)	Length
1	4.2333×10^{-2}	2.3375×10^{-2}
2	3.5643×10^{-3}	2.3124×10^{-2}
3	4.2179×10^{-4}	1.2431×10^{-2}
4	7.9549×10^{-5}	1.2065×10^{-2}
5	1.0260×10^{-5}	2.7588×10^{-3}
6	1.1721×10^{-6}	2.6928×10^{-3}

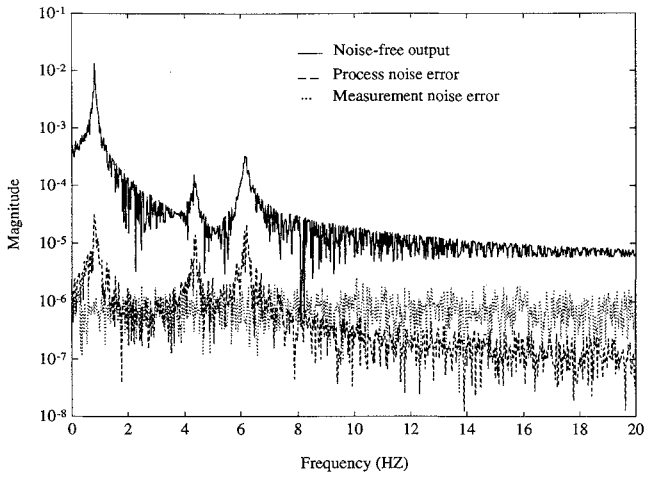

Fig. 5 Error from process and measurement noise.

Parametric Uncertainty Estimation

The algorithm developed in this paper for the parametric uncertainty estimation is discussed in this section. First recall that the measurement is random input response of the actual model with process and measurement noises.

Figure 5 shows the magnitude plots of the DFT of the output of the noise-free model, the DFT of the output error contributed from the process noise, and the DFT of the output error contributed from the measurement noise. The error around the natural frequencies of the three identified modes is mainly contributed from the process noise. The error from measurement noise has spectrum uniformly distributed throughout the frequency range. The error in the high-frequency range and the valley parts of the identified transfer function is mainly contributed from the measurement noise.

The OKID is applied to identify a nominal model from the noisy input/output data. In Ref. 17, we have shown that the OKID can identify a very accurate model with a negligible model error from noise-free random input response date. Figure 6 shows the magnitudes of the OKID-identified model g^0 and the estimated model error g_e. Figure 6 also shows the magnitude of the model spectral difference between the actual model g and the identified model g^0.

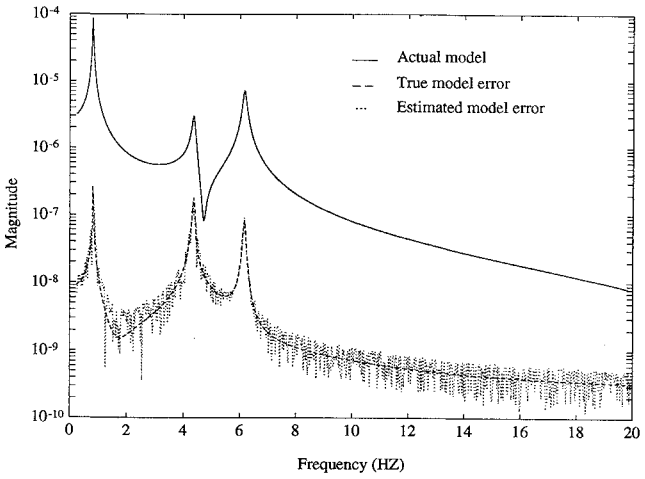

Fig. 6 Identified model and model error.

In practice, the actual model cannot be identified from noisy input/output data. Here it is only used as reference. The magnitude of the estimated model error g_e is around 10 times larger than the magnitude of the model difference in the frequency ranges around the three natural frequencies. The model error g_e has peaks close to the three natural frequencies. As discussed earlier, we have chosen the flat error in the high-frequency range and the valley parts of the identified transfer function as the nonparametric error. The error transfer function, which is used to bound the nonparametric error, is chosen as a constant

$$\Delta G(z) = 5 \times 10^{-8}$$

This error transfer function $\Delta G(z)$ bounds the model error in the following portions: 1) frequency lower than 0.5 Hz, 2) valley portions of identified model, and 3) frequency higher than 7 Hz. The corresponding continuous error transfer function $\Delta G_s(s)$ obtained by using the bilinear transformation is identical to $\Delta G(z)$.

The parametric error is determined to cover the error in frequencies around the three natural frequencies and where the magnitude of g_e is larger than $5. \times 10^{-8}$. There are 35 frequency points ($N_p = 35$) chosen for the parametric uncertainty estimation with the order of the transfer function numerator being 5. Table 1 shows the results of the discrete-interval model of model structure 1.

From Table 1, the following observations are noted:

1) The actual model and the identified model both belong to the interval model.

2) The length of each interval, $p^+(i) - p^-(i)$, is about one order larger than the corresponding model difference, $|p(i) - p^0(i)|$. This is consistent with the results in Fig. 6.

In this Mini-Mast example, six transfer function denominator coefficients are considered as parameters and the dimension of the error vector Δd_i is 6. Actually, the error vector Δd_i may be dominated by

Table 3 Discrete model structure 2

	β_i^-	β_i^+	Δq_i^0	SVD($\mathbf{\Delta}_d$)
$q_1(z)$	-2.157×10^{-2}	1.579×10^{-2}	-3.617×10^{-3}	4.233×10^{-2}
$q_2(z)$	-1.481×10^{-3}	1.335×10^{-3}	-2.739×10^{-4}	3.564×10^{-3}
$q_3(z)$	-1.467×10^{-4}	1.507×10^{-4}	-3.776×10^{-5}	4.218×10^{-4}
$q_4(z)$	-4.249×10^{-5}	3.157×10^{-5}	1.044×10^{-5}	7.955×10^{-5}
$q_5(z)$	-5.950×10^{-6}	2.483×10^{-6}	8.163×10^{-7}	1.026×10^{-5}
$q_6(z)$	-7.735×10^{-7}	3.584×10^{-7}	-6.554×10^{-8}	1.172×10^{-6}
	α_i^-	α_i^+	Δr_i^0	SVD($\mathbf{\Delta}_n$)
$r_1(z)$	-2.290×10^{-8}	1.131×10^{-8}	2.563×10^{-9}	3.506×10^{-8}
$r_2(z)$	-8.153×10^{-10}	1.158×10^{-9}	3.028×10^{-11}	1.677×10^{-9}
$r_3(z)$	-3.056×10^{-10}	2.752×10^{-10}	-2.141×10^{-11}	6.182×10^{-10}
$r_4(z)$	-2.671×10^{-11}	2.012×10^{-11}	2.176×10^{-12}	6.171×10^{-11}
$r_5(z)$	-1.302×10^{-11}	8.557×10^{-12}	3.498×10^{-12}	2.500×10^{-11}
$r_6(z)$	-4.417×10^{-12}	5.962×10^{-12}	-5.938×10^{-13}	1.560×10^{-11}

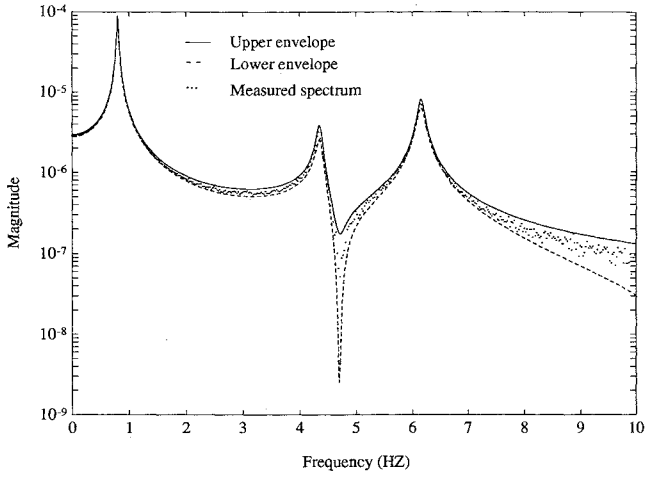

Fig. 7 Interval system with error bound transfer function and estimated spectrum.

a lower order dimension. To discuss this phenomenon, we compare the singular values of $\mathbf{\Delta}_d$ and the interval lengths of the denominator part. Table 2 shows the singular values and the interval lengths listed in descending order. From Table 2, the ratio between the largest interval length and the smallest interval length is less than 10. The singular values of $\mathbf{\Delta}_d$ drop dramatically and the largest singular value of $\mathbf{\Delta}_d$ is about five orders larger than the smallest singular value of $\mathbf{\Delta}_d$. Actually, the denominator parameter error is dominated by the error in the directions of the first three singular vectors of $\mathbf{\Delta}_d$. The model uncertainty in the directions of the last three singular vectors is negligible. Based on the above analysis, using model structure 1 to represent the parametric uncertainty seems to be conservative. To improve this parametric uncertainty estimation, model structure 2 is generated by using the SVD technique discussed earlier. Table 3 shows the results of model structure 2.

In Table 3, Δq_i^0 and Δr_i^0 represent the corresponding parameters of the true model difference $\Delta \boldsymbol{p}^0$ $(= \boldsymbol{p} - \boldsymbol{p}^0)$. The parameters Δq_i^0 and Δr_i^0 are always inside the corresponding intervals. It means that the actual model belongs to the interval model. The results for the continuous interval models for both model structures can be found in Ref. 17. Here we apply the edge theorem[9] to find the magnitude envelopes of the discrete-interval model based on the model structure 2.[10] Figure 7 shows the magnitude envelopes and the magnitude of the estimated spectrum $\hat{g}$. The solid line in Fig. 7 is the sum of the maximum magnitude of the interval model and $|\Delta G|$. The dashed line is the difference between the minimum magnitude of the interval model and $|\Delta G|$. The dotted line is the magnitude of $\hat{g}$. Figure 7 clearly shows that the envelopes precisely bound the magnitude of $\hat{g}$. We also apply the edge theorem to obtain the boundary of the poles of the discrete-interval model. These results are shown in Fig. 8. In these figures, the star represents the eigenvalues of the identified models $\boldsymbol{p}^\nu$ and the dot represents the boundaries of the eigenvalues of the interval model. Each eigenvalue boundary of the interval model precisely covers the corresponding eigenvalues of the identified models. The results for the boundaries of the eigenvalues of the continuous interval model for model structure 2 can be found in Ref. 17.

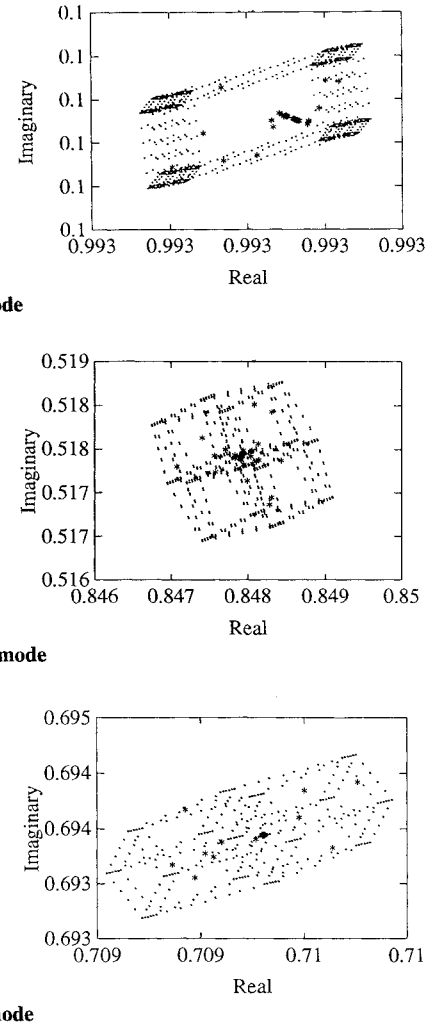

Fig. 8 Root clusters of discrete-interval model and eigenvalues of identified models.

Model structure 3 can be generated by using the ranges of coefficients of the partial fractions of the transfer functions for all identified models $\boldsymbol{p}^\nu$ $(\boldsymbol{p}_s^\nu)$. This kind of continuous interval model represents the ranges of dampings and natural frequencies of the

identified modes.[17] It gives a physical representation of the parametric uncertainty.

Concluding Remarks

This paper presents an algorithm to quantify the model error in the frequency domain in terms of parametric and nonparametric uncertainties. Unlike the H_∞ approach, the model error around the natural frequencies of the identified modes is considered as the parametric uncertainty.

Three different model structures are discussed in this paper to represent the parametric uncertainty. The interval model based on model structure 1 is represented as the intervals of the transfer function coefficients and it is a straightforward one. The computational effort of applying a frequency-domain tool to this type of interval model is minimum. The interval model based on model structure 2 is developed to reduce the conservativeness of the interval model from model structure 1. This interval model captures the estimated parameter errors in a much less conservative way. The interval model based on model structure 3 represents the interval system of physical parameters. Future studies are to experimentally verify the algorithm developed in this paper and to extend it to multi-input and multi-output systems. Another possible study is to apply the algorithm to quantify the μ structural uncertainty for the H_∞ control design.

Acknowledgments

This research is supported in part by NASA Grant NAG 5-2109 and National Science Foundation Grant HRD-9252932. These supports are gratefully acknowledged.

References

[1]Bayard, D. S., Hadaegh, F. Y., Yam, Y., Scheid, R. E., Mettler, E., and Milman, M. H., "Automated On-Orbit Frequency Domain Identification for Large Space Structures," *Automatica*, Vol. 27, No. 11, 1991, pp. 931–946.

[2]Helmicki, A. J., Jacobson, C. A., and Nett, C. N., "Control Oriented System Identification: A Worst-Case/Deterministic Approach in H_∞," *IEEE Transactions on Automatic Control*, Vol. AC-36, No. 10, 1991, pp. 1163–1176.

[3]DeVries, D. K., and Vandenhof, P., "Quantification of Model Uncertainty from Experimental Data," *Selected Topics in Identification, Modelling, and Control*, Vol. 4, Delft Univ. Press, The Netherlands, 1992, pp. 1–10.

[4]Younce, R. C., and Rohrs, C. E., "Identification with Nonparametric Uncertainty," *IEEE Transactions on Automatic Control*, Vol. AC-37, No. 7, 1992, pp. 715– 728.

[5]Pappa, R. S., Schenk, A., and Noll, C., "ERA Model Identification Experiences with Mini-Mast," *Proceedings of the Second USAF/NASA Workshop on System Identification and Health Monitoring of Precision Space Structures*, Pasadena, CA, March 1990.

[6]Kharitonov, V. L., "Asymptotic Stability of an Equilibrium Position of a Family of Systems of Linear Differential Equations," *Differential Uravnen*, Vol. 14, 1978, pp. 2086–2088.

[7]Chapellat, H., and Bhattacharyya, S. P., "A generalization of Kharitonov's Theorem: Robust Stability of Interval Plants," *IEEE Transactions on Automatic Control*, Vol. AC-34, No. 3, 1989, pp. 306–311.

[8]Bhattacharyya, S. P., and Keel, L. H., "Robust Stability and Control of Linear and Multilinear Interval Systems," *Control and Dynamic Systems*, Vol. 51, Academic, New York, 1992, pp. 31–78.

[9]Bartlett, A. C., Hollot, C. V., and Lin, H., "Root Location of an Entire Polytope of Polynomials: It Suffices to Check the Edges," *Mathematics of Controls, Signals and Systems*, Vol. 1, 1988, pp. 61–71.

[10]Bhattacharyya, S. P., Chapellat, H., and Keel, L. H., *Robust Control: The Parametric Approach*, Prentice-Hall, Englewood Cliffs, NJ, 1994.

[11]Keel, L. H., Lew, J.-S., and Bhattacharyya, S. P., "System Identification Using Interval Dynamic Models," *Proceedings of the 1994 American Control Conference* (Baltimore, MD), Inst. of Electrical and Electronics Engineers, Piscataway, NJ, 1994.

[12]Juang, J.-N., Phan, M., Horta, L. G., and Longman, R. W., "Identification of Observer/Kalman Filter Markov Parameters: Theory and Experiments," *Journal of Guidance, Control, and Dynamics*, Vol. 16, No. 2, 1993, pp. 320–329.

[13]Juang, J.-N., Phan, M., and Horta, L. G., "User's Guide for System/Observer/Controller Identification Toolbox," NASA TM-107566, 1992.

[14]Kosut, R. L., "On-Line Identification and Control Tuning of Large Space Structures," *Proceedings of the 1987 American Control Conference*, Minneapolis, MN, June 1987.

[15]Klema, V. C., and Laub, A. J., "The Singular Value Decomposition: Its Computation and Some Application," *IEEE Transactions on Automatic Control*, Vol. AC-25, No. 2, 1980, pp. 164–176.

[16]Bayard, D. S., Yam, Y., and Mettler, E., "A Criterion for Joint Optimization of Identification and Robust Control," *IEEE Transactions on Automatic Control*, Vol. AC-37, No. 7, 1991, pp. 986– 990.

[17]Lew, J.-S., Keel, L. H., and Juang, J.-N., "Quantification of Model Error via an Interval Model with Nonparameter Error Bound," *Proceedings of the 1993 AIAA Guidance, Navigation, and Control Conference* (Monterey, CA), AIAA, Washington, DC, 1993.